SH33A-2036

The Rising Phase of Solar Cycle 24: General Solar Wind, Large-Scale Solar Wind Structures, and Sector Asymmetry

L.K. Jian[1], C.T. Russell[1], J.G. Luhmann[2], P. Riley[3], J.T. Hoeksema[4], D. Odstrcil[5,6], G. Petrie[7]

[1]Inst. Geophysics & Planetary Physics, Dept. Earth & Space Sciences, UC Los Angeles, CA, USA (*lanjian@ucla.edu*) [2]Space Sciences Lab., UC Berkeley, CA, USA

[3]Predictive Science, Inc., CA, USA [4]Standford Univ., CA, USA [5]Goddard Space Flight Center, NASA, MD, USA [6]George Mason Univ., VA, USA [7]National Solar Observatory, NM, USA

1. Solar Background

From the long-term observations of Wilcox Solar Observatory (WSO), the polar magnetic field of the Sun at solar minimum has been weakening since solar minimum 21/22 (**Figure 1**). After the minmum 23/24, the average polar field gradually decreases and approaches to the field reserval. In 2011, the approach slows down, becoming more gradual than the approach of solar maximum in cycles 21-23. Hence, ***the solar maximum 24 could still be one or two years away***.

In late 2011, the computed tilt angle of heliospheric current sheet (HCS) increased to 71° (**Figure 2**). If the maximum tilt will reach 75° at this maximum, similar to the previous solar maxima, it is likely to take one year or more to reach. However, it is also possible that the maximum tilt of HCS during solar maximum 24 would differ than during maxima 21-23, depending on the strengths of quadrupole and hexapole fields. In addition, from **Figure 2**, we note the potential field source surface (PFSS) model using source surfaces at different heliocentric distances gives different tilt angles of the HCS, especially for solar minima.

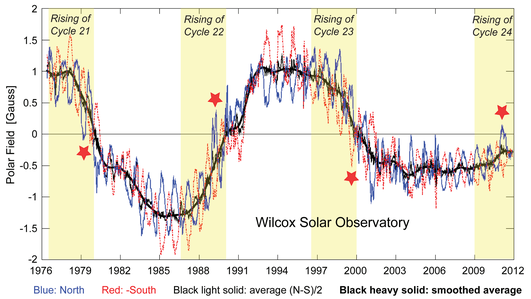

Figure 1. Variations of solar polar field from May 1976 to November 2011, measured in the poleward 3' apertures at WSO. Each 10 days, the usable daily polar field measurements in a centered 30-day time window are averaged. Yearly geometric projection effects are eliminated by a 20 nHz low pass filter. Red stars mark first field reversals of the dominant polarities in rising phases. After that, it took one year or so for the average field to reverse in cycles 21-23. Courtesy of WSO.

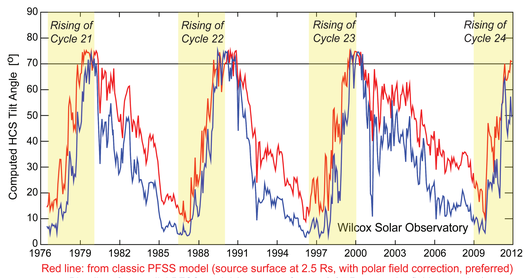

Figure 2. Variations of Carrington-rotation averages of HCS tilt angle over May 1976 - October 2011 from WSO. The maximum latitudinal extent of the HCS was computed using "classic" or radial potential field models applied to WSO photospheric magnetic field observations. Different heliocentric distances are used for source surfaces. Courtesy of WSO.

Acknowledgements: This work is supported by NASA's STEREO program through Grant NAS5-03131 administered by UC Berkeley, and NSF SHINE program through Award AGS-1062105. We thank all the PIs for making the data available. We acknowledge all the people who have constructed and maintained the OMNI data in NASA/SPDF. We thank Robert Lin and Linghua Wang for provding the SEP flux data of Wind/3DP.

JLK-2011-Nov 29-AGU

2. Solar Wind and Geomagnetic Activity

Figure 3 displays the 27-day averages of sunspot number (SSN), solar wind parameters, and geomagnetic activity indices. The SSN reached 80 in 2011, which is the level of middle 1998. During the rising phase of solar cycle 24, the flux of solar energetic protons (SEP) is significantly weaker than during the previous rising phase, at both energy ranges of 0.7-7 MeV and 6-11 MeV. No SEPs of energy > 10 MeV have been observed at L1 yet for this cycle. This indicates the ***solar activity is significant weaker than previous cycle***.

In comparison with the previous rising phase, the present IMF is still below 6 nT, lower than the late 1997. In contrast with the symmetric oscillation of Br around 0 during 1996.5-1998.5, the 27-day average of Br was asymmetric and mostly inward in 2009-2010, and changed to outward in 2011. In comparison with the previous rising phase, the *north-south component of IMF (Bz) in GSM coordinates is weaker and has lower occurrence of southward direction at this rising phase except the last few data points*.

The solar wind density and dynamic pressure are noticeably lower in this rising phase. In 2011, the solar wind speed and temperature reached the level of 1998-1999. The dawn-dusk component of electric field (Ey) in 2009-2011 was slightly weaker than the last rising phase except the very recent rise. Due to the *less active Sun* and *weaker solar wind dynamic pressure and Ey*, the *geomagnetic activity represented by Ap and Dst indices in this rising phase is much weaker than in the previous one*.

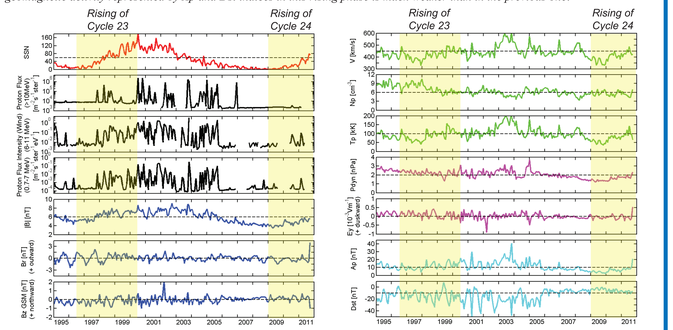

Figure 3. Variations of solar background, solar wind, and geomagnetic activity from 1995 to present. The 27-day averages of OMNI data from NASA/SPDF are used. From top to bottom: SSN, solar protons of energies > 10 MeV, solar protons of 6-11 MeV measured by Wind/3DP (at ecliptic longitude 18-54^{0} North and South), solar protons of 0.7-7 MeV from Wind/3DP (full 3-D proton observations up to 6 MeV), IMF magnitude, radial field, north-south IMF component in GSM coordinates, solar wind speed, proton number density, proton temperature, dynamic pressure, dawn-dusk component of electric field, Ap index indicating the changes of magnetic field arising from the Earth's mid-latitude ionospheric current systems, and Dst index indicating the strength of longitudinally-averaged depression in the geomagnetic field at the equator mainly due to ring current. Refer to OMNIWeb for data sources of individual parameters.

3. Stream Interaction Regions (SIRs) and Interplanetary CMEs (ICMEs)

A SIR is formed by a fast wind stream overtaking a preceding slow wind stream. SIRs include corotating interaction regions (CIRs) and transient or localized stream interactions which do not last more than one solar rotation. We require 5 of the following signatures to be a SIR: overall speed increase, velocity deflection, pile-ups of magnetic field and total pressure Pt (the sum of magnetic pressure and plasma thermal pressure), increase and then decrease of solar wind density, increase of solar wind temperature, change of entropy.

An ICME is an interplanetary couterpart of CME. ICMEs have various characteristics: field enhancement, smooth field rotations, quiet field, low temperature, low β, increase of α particle abundance, Pt enhancement, declining solar wind speed, bidirectional suprathermal electrons. None of these features is unique to ICME, so we require 3 of them to be an ICME.

Figures 4-6 illustrate the annual averages of SIR, ICME, and interplanetary shock properties from 1995 to 2010. The statistics of 1995-2009 are based on Wind/ACE observations while the results of 2010 are based on STEREO A/B observations. In comparison with the rising phase of cycle 23, SIRs in this rising phase ***occur more often, with a higher recurrence rate*** (due to fewer transient disturbances) and a similar shock rate. Similar to the previous rising phase, the mean speed, speed increase, maximum field, and maximum Pt all increased from 2009 to 2010, but the field and Pt were weaker than previous rising phase.

ICME occurrence rate and shock rate rose from 2009 to 2010, but the rates were lower than in the last rising phase. Similar to the rising phase of cycle 23, the ICME parameters have all increased since 2009. However, the ***ICMEs in this rising phase are smaller and slower, and their expansion speed is slower***. The peak field and Pt in 2009 and 2010 are remarkably weaker than in the last rising phase. The SIR-driven shocks are much weaker in this rising phase than previous one. The rate and proxy strength of ICME-driven shocks increased in 2009-2010, but they are still considerably lower than the last rising phase.

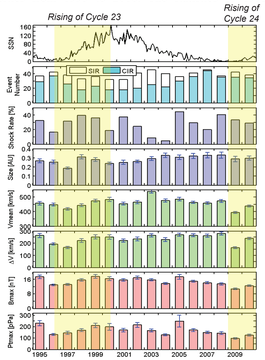

Figure 4. Variations of the annual average SIR properties during 1995-2010: monthly SSN, event number of SIRs (white) and CIRs (light blue), shock association rate, size, mean speed (average of maximum and minimum speed within a SIR), speed increase over a SIR, maximum field, maximum Pt. The error bar indicates the probable error of the mean. Extended after *Jian et al. (2011)*.

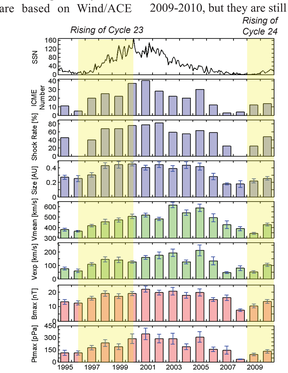

Figure 5. Variations of the annual average ICME properties from 1995 to 2010. From top to bottom: monthly SSN, ICME number, shock association rate, size approximated by the product of duration and mean speed, mean speed, expansion speed, maximum field, maximum Pt. The error bar denotes the probable error of the mean. Extended after *Jian et al. (2011)*.

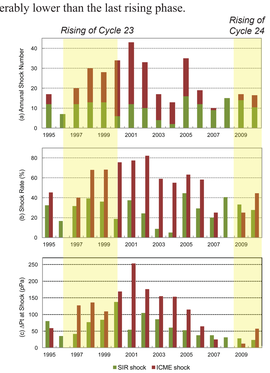

Figure 6. Variations of the annual shock properties from 1995 to 2010. From top to bottom: shock event number, shock rate of SIRs/ICMEs, shock strength approximated by the change of Pt at the shock. Green bars for SIR-driven shocks, red bars for ICME-driven shocks. Extended after *Jian et al. (2011)*.

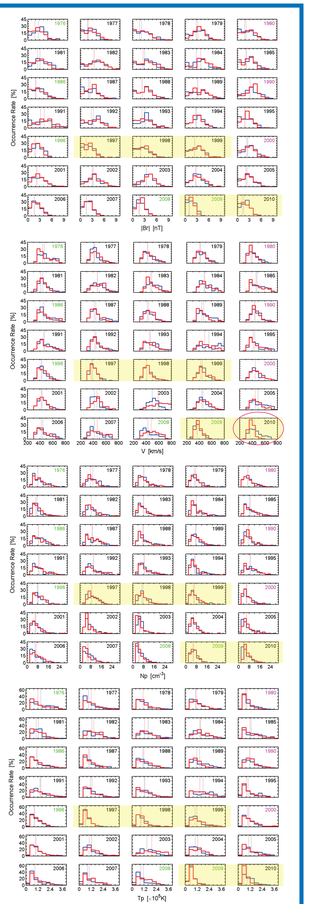

Figure 9. From top to bottom: the histograms of Br magnitude, solar wind speed, proton number density, and proton temperature for +(red) and -(blue) sectors over 1976-2010. Daily-averaged OMNI data are used. *These histograms are similar to the ones using +/- Br as indicators.* The red and blue vertical dashed lines denote the annual averages for + and - sectors. Light yellow boxes mark the rising phases of cycles 23 and 24.

4. North-South Asymmetry in Solar Wind and IMF

Figure 7 shows the solar cycle variations of the occurrence rates of positive field polarity from OMNI observations. (1) +/- Br are not observed at equal rate for most of the years, as also noted by Hiltula and Mursula (2007), Erdos and Balogh (2010). Only considering years since 1995 when continuous observations at L1 became available, the most asymmetric year is 2009, with + polarity (currently from southern hemisphere) observed about 60% of the time. (2) Shown by the red and green lines, **+ polarity is observed more often at 1 AU than - polarity in odd cycles (21, 23), vice versa in even cycle (22)**. (3) The dominant polarities by counting daily Br data or using sector boundaries are similar each year. (4) The cumulative field over 1976-2010 is nearly symmetric, while the cumulative field from the PFSS model is a little asymmetric (**Table 1**), probably because the total pressure always tries to reach a balance between two hemispheres as the solar wind expands. Since 2007, the - polarity has been dominant in observations. In 2009, its dominance reached the highest since 1995 and is now weakening.

Figure 8 illustrates the latitudinal distributions of Br and solar wind speed V from 1976 to 2010. The Br distribution changes its tilt at each solar minimum. At solar min 23/24, the Br<0 occurred at a wider range of helio-latitudes, consistent with dominant - polarity in **Figure 7**. The latitudinal distribution of Br is more symmetric near solar maxima than at other times. The latitudinal distribution of V has no clear variation trend. The latitude range of slow wind is wider at solar minima. In 2008-2009, the solar wind is faster at south latitudes than at north latitudes.

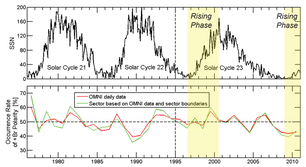

Figure 7. Variations of (top) montly SSN and (bottom) annual occurrence rates of positive polarity of Br during 1976-2010. *The sector boundary identification requires a uniform field polarity of at least 4 days at either side of the boundary.* OMNI data had many data gaps before 1995.

Table 1. Summary of Field Asymmetry over 1976-2010

Category	Br>0 [%]	Br<0 [%]
OMNI Daily Data	49.4	50.6
Sectors	49.3	50.7
PFSS Model at 2.5 Rs	47.8	52.2
PFSS Model (2.5 Rs before CR 1870, 1.8 Rs since CR 1870)	47.3	52.7

Figure 9 displays the histograms of Br magnitude, V, proton number density, and proton temperature of the + and - sectors from 1995 to 2010. (1) Br magnitudes from the two sectors do not differ much at solar minima except in 1976 when there were too many data gaps. Currently, Br magnitude from - sector is slightly stronger (by < 0.5 nT) than + sector. In contrast, IMF magnitudes from +/- sectors do not differ much at solar minima, and they are close to each other in recent years (not shown). (2) The asymmetry of V between +/- sectors is most significant in 2003, with the difference of 100 km/s, probably because of many superfast CMEs in 2003. From 2008 to 2010, V from - sector becomes faster than the one from + sector, and the discrepancy between the two sectors is ~100 km/s. (3) Proton density from +/- sectors differ not much throughout the years, especially at solar minima. The largest difference occurred in 1977 and 2010, by ~ 2 cm^{-3}. (4) Proton temperature from +/- sectors varies similarly to V. From 2008 to 2010, the solar wind from - sector becomes hotter than the wind from + sector.

Summary of the Poster

From WSO records, the approach of polar field reversal is slower in this rising phase than the rising phases of cycles 21-23. We may need to wait one or two more years to reach solar maximum. In the current rising phase, the solar activity, IMF, solar wind dyanimc pressure and electric field, SIRs, ICMEs, and shocks are weaker than the rising phase of cycle 23.

The dominant field polarity changes from cycle to cycle. The asymmetry of plasma parameters between + and - sectors do not have clear solar cycle dependence. In comparison with previous rising phase, the N-S asymmetry is ***more pronounced*** in this rising phase. The negative polarity is likely to be observed more often in cycle 24. Currently, the solar wind from northern hemisphere (- sector) is faster and hotter, has stronger Br and smaller proton density than the wind from southern hemisphere. This can affect the geomagnetic activity systematically.

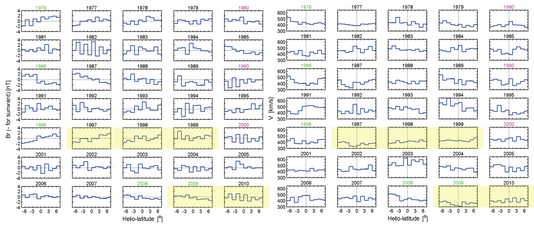

Figure 8. Helio-latitudinal distributions of Br and solar wind speed V from 1976 to 2010, based on daily-averaged OMNI data. Magenta indicates years at solar maxima, while green for years at solar minima. Light yellow boxes mark the rising phases of cycles 23 and 24.